JOURNAL OF AGRICULTURAL AND FOOD CHEMISTRY

Agricultural and Environmental Chemistry

Design, Herbicidal Activity, and QSAR Analysis of Cycloalka[d]quinazoline-2,4-dione-Benzoxazinones as Protoporphyrinogen IX Oxidase Inhibitors

Da-Wei Wang, ruibo zhang, Ismail Ismail, Zhiyuan Xue, Lu Liang, Shuyi Yu, Xin Wen, and Zhen Xi

J. Agric. Food Chem., **Just Accepted Manuscript** • DOI: 10.1021/acs.jafc.9b02996 • Publication Date (Web): 29 Jul 2019

Just Accepted

is published by the American Chemical Society. 1155 Sixteenth Street N.W., Washington, DC 20036

Design, Herbicidal Activity, and QSAR Analysis of Cycloalka[*d*]quinazoline-2,4-dione−Benzoxazinones as Protoporphyrinogen IX Oxidase Inhibitors

Da-Wei Wang,[#] Rui-Bo Zhang,[#] Ismail Ismail, Zhi-Yuan Xue, Lu Liang, Shu-Yi Yu, Xin Wen, and Zhen Xi*

State Key Laboratory of Elemento-Organic Chemistry, and Department of Chemical Biology, National Pesticide Engineering Research Center, Collaborative Innovation Center of Chemical Science and Engineering, College of Chemistry, Nankai University, Tianjin 300071, P. R. China.

*corresponding author: E-mail: zhenxi@nankai.edu.cn (Z. Xi), Tel: +86 022-23504782. Fax: +86 022-23504782.

[#]D.-W. W. and R.-B. Z. contributed equally to this work.

Abstract:

In continuation of our search for potent protoporphyrinogen IX oxidase (PPO, EC 1.3.3.4) inhibitors, we designed and synthesized a series of novel herbicidal cycloalka[*d*]quinazoline-2,4-dione-benzoxazinones. The bioassay results of these synthesized compounds indicated that most of the compounds exhibited very strong *Nicotiana tabacum* PPO (NtPPO) inhibition activity. More than half of the 37 synthesized compounds displayed over 80% control of all three tested broadleaf weeds at 37.5-150 g ai/ha by post-emergent application, majority of them showed no phytotoxicity toward at least one kind of crop at 150 g ai/ha. Promisingly, **17i** (K_i = 6.7 nM) showed 6 and 4 times more potent than flumioxazin (K_i = 46 nM), and trifludimoxazin (K_i = 31 nM), respectively. Moreover, **17i** displayed excellent and broad-spectrum herbicidal activity even as low as 37.5 g ai/ha, and safe for wheat at 150 g ai/ha by post-emergent application, indicating the great potential for **17i** development as a herbicide for weed control in wheat fields.

KEYWORDS: benzoxazinone; cycloalka[*d*]quinazoline-2,4-dione, protoporphyrinogen IX oxidase; herbicide; weed control

Introduction

Protoporphyrinogen IX oxidase (PPO, EC 1.3.3.4) is one of the most important targets for herbicide discovery, catalyzes the oxidation of protoporphyrinogen IX to protoporphyrin IX.[1-3] *In planta*, protoporphyrin IX is the substrate for the biosynthesis of chlorophyll, which is a key pigment for photosynthesis. Inhibition of PPO can lead to the toxic accumulation of protoporphyrin IX in the cytoplasm, upon exposing to light it generates reactive oxygen species, which, in turn, result in cell death and plants bleaching.[4-7] Therefore, PPO herbicides are also called peroxidizing herbicides. The research of PPO herbicides was initiated in the 1960s, peaked around the 1990s and decreased soon due to the development of genetically modified glyphosate-resistant crops, such as glyphosate-resistant soybeans.[8] This weed populations resistance has resulted because of the overuse of some herbicides. PPO-inhibiting herbicides can effectively control some triazine-, AHAS- and glyphosate-resistant weed biotypes.[9] Most interestingly, even share the same mode of action, some newly developed PPO inhibitors can also suppress the PPO herbicides-resistance *Amaranthus* biotypes.[10] As a consequence, in recent years, the discovery of new PPO inhibitors has again been a very active research area for the agrochemical industry.[11]

To date, there are thousands of PPO inhibitors have been reported in the literature, about 30 of them currently used as herbicides to decimate weeds in fields.[12,13] Depending on the structural features, many PPO herbicides have hydrophobic side chains to increase the foliar absorption and translocation in plants, some of them even shared the similar core skeleton (Figure 1). For example, saflufenacil, butafenacil and tiafenacil all belong to pyrimidinedione type inhibitors, the different hydrophobic warheads in their structures, which, not only make them easier absorb by foliage and transfer in whole plants, but also can improve the binding affinity of them with plants

PPOs.[14, 15] According to the PPO herbicides classification methodologies, flumioxazin (*N*-phenyl-phthalimides), thidiazimin (thiadiazoles), and trifludimoxazin (triazinones) belong to different types of herbicides.[12] However, they all bearing the benzoxazinone skeleton as the core motif, and the benzoxazinone systems are connected with heterocyclic moieties via the C-N bond. Flumioxazin is one of the most widely used PPO herbicides, showing excellent broad-spectrum of herbicidal activity including these AHAS- and glyphosate-resistant *Amaranthus* weeds.[15] Thidiazimin is an effective contact herbicide for dicotyledonous weeds control in winter cereals. Trifludimoxazin is the first triazinone-containing PPO herbicide with a novel mechanism of action.[10] It shows quick burn-down action against the leaves of weeds with one day. What makes trifludimoxazin unique is that it can effectively suppress some PPO-resistant biotypes such as *Amaranthus spp.* and *Ambrosia spp.*

The reported studies show that it is an effective approach to obtain a new compound with improved bioactivities by placing the heterocyclic moieties at the 6-position of benzoxazinone ring. [16-18] Roy K. and Paul S. have found that the electrostatic potential surface of the heterocyclic moieties of benzoxazinone derivatives is crucial to bioactivities.[17] Compounds with the electrostatic positively charged surface at this position were found to showed better activity, whereas, inhibitors with negatively charged surface were proved detrimental to PPO-inhibiting activity. To date, PPO inhibitors are designed by mimicking part of the enzyme substrate protoporphyrinogen IX.[12] We have found that the protoporphyrinogen IX bound to the active site of *Nicotiana tabacum* PPO (NtPPO) with two pyrrole rings buried in the bottom of the pocket, and two carboxyl groups orientated to the product channel.[19] The catalytic pocket of PPO is mainly formed by a number of hydrophobic residues, such as Leu334, Phe392, Leu372, and Leu356, indicating that compounds with hydrophobic groups may be advantageous to

PPO-inhibiting activity. Based on the above-mentioned studies, we thought that integrated hydrophobic and heterocyclic moieties and benzoxazinone system into a molecular architecture would promote the discovery of novel PPO inhibitors with improved activity. Cycloalkanes and pyrimidine-2,4(1*H*,3*H*)-dione are biologically important functional scaffolds exist in many natural products, agrochemicals, and pharmaceuticals.[20-22] Previously, we have reported a series of pyridopyrimidine-2,4-dione−benzoxazinones, the results showed that the fluorine atom was the optimal substituent at the 7-position of the benzoxazinone ring.[23] As a continuation of our program to search for novel PPO inhibitors, herein, a novel series of cycloalka[*d*]quinazoline-2,4-dione-benzoxazinones possessing a fluorine atom at the 7-position of benzoxazinone system were designed and synthesized (Figure 2). The NtPPO inhibitory activity, structure-activity relationships (SAR), herbicidal activity, and crop selectivity of the newly synthesized compounds were systematically explored.

MATERIALS AND METHODS

Preparation of cycloalka[*d*]quinazoline-2,4-dione-benzoxazinones 8, **9**, **17**, and **19**. The synthetic routes for **8**, **9**, **17**, and **19** are shown in Scheme 1-3, the detailed synthetic methods, characterization data (^{1}H and ^{13}C NMR, HRMS, melting point) of the compounds are shown in the Supporting Information.

X-ray Diffraction. The single crystals of compound **17a** were obtained by slow evaporating from chloroform solution. The supplementary crystallographic data for **17a** had been deposited in the Cambridge Crystallographic Data Centre (CCDC, http://www.ccdc.cam.ac.uk/), the deposition number is 1911322. The crystal structure of **17a** is shown in Figure 3.

PPO Inhibitory Experiments. The expression and purification of *Nicotiana tabacum*

mitochondrial PPO2 (NtPPO) were performed as described previously.[23-25] The enzyme substrate protoporphyrinogen IX was synthesized by reduction of protoporphyrin IX with freshly prepared sodium amalgam. Due to the chemical nature of protoporphyrin IX, it has a maximum excitation at 410 nm and a maximum emission of 630 nm. In the kinetic inhibition assays, we used a fluorescence detector to monitor the formation of the protoporphyrin IX by setting the emission wavelengths to 631 nm and excitation wavelengths to 410. Inhibitors were dissolved in dimethyl sulfoxide (DMSO) as stock solution, and diluted to the different concentration ranges from 0.05 μM to 50 mM just before using. The total volume of reaction solution was 200 μL, which consists of 0-40 μg PPO, 5 μM flavin adenine dinucleotide (FAD), 5 mM DTT, 1 mM EDTA, 0.2 M imidazole, 0.1 M potassium phosphate buffer (pH 7.4), and 0.03% Tween 80 (v/v). To initiate the PPO reaction, 0-6.5 μM protoporphyrinogen IX was added to the assay solution.

The half maximal inhibitory concentration (IC_{50}) value of inhibitors was calculated by fitting v versus [I] data to a single binding site model (eq 1). The kinetic parameters were calculated by Sigma Plot software 10.0 (SPSS, Chicago, IL).

$$y = \min + \frac{\max - \min}{1 + 10^{\log IC_{50} - x}} \quad (1)$$

in this equation, y is the percentage of the maximal rate, min and max being the y values at which the curve levels off, x is the logarithm of inhibitor concentration. The inhibition constant of the enzymatic reaction (K_i) was calculated by using the following relationship among IC_{50}, K_i, and K_m (1.52 μM) at any saturated substrate concentration (eq 2). The results of K_i values of inhibitors are shown in Table 1.

$$K_i = \frac{IC_{50}}{S/K_m + 1} \quad (2)$$

Molecular Modeling and 3D-QSAR Analysis. The structure of NtPPO (PDB ID: 1SEZ) was

downloaded and prepared by standard methods using Autodock Tools Package before docking.[26] The 3D structures of cycloalka[*d*]quinazolinedione−benzoxazinones were constructed by SYBYL-X 6.9 (Tripos, Inc., St. Louis, MO) based on the crystal structure of **17a**, and subsequently optimized with the conjugate-gradient and steepest-descent algorithm to a convergence criterion of 0.005 kcal/mol. Docking calculations of two molecules were performed on AutoDock4.2 by using a genetic algorithm, for each ligand the docking runs were set to 500. After calculation, the results were clustered, and the best binding modes were selected by the docking energy as well as by comparison with the co-crystal ligand.[27] The binding free energies of **8i** and **9i** with NtPPO were calculated by molecular mechanics-Possion-Boltzmann surface area (MM-PBSA) method, and the results are shown in Table S1. Open3DAlign was used to align the 36 synthesized molecules, the best align mode was selected both referred to the docking modes and the crystal structure of **17a**, then the aligned compounds were transferred to Open3DQSAR to build the QSAR model.[28] A grid box with 5.0 Å margin and 0.5 Å step size was set around the compounds. The compounds number for training and test sets were 28 and 8, respectively. Electrostatic potential and steric factors of molecular interaction fields was then calculated, other parameters used for the calculation were the same as described by Tosco et al.[29] The experimental and predicted activity values are depicted in Table 2, and PyMOL was used to visualize the QSAR results.

Herbicidal activity. The post-emergence herbicidal activity of compounds **8**, **9**, **17**, and **19** against three dicot weeds, *Eclipta prostrata* (*E.p.*), *Abutilon juncea* (*A.j.*), and *Amaranthus retroflexus* (*A.r.*); and three monocotyledonous weeds, *Setaria faberii* (*S.f.*), *Digitaria sanguinalis* (*D.s.*), and *Echinochloa crusgalli* (*E.c.*) were evaluated by using the similar reported procedures.[30-35] To further evaluate the herbicidal spectrum bioactivities of compounds **8i**, **9i** and

17i, another thirteen weeds: *Ipomoea nil* (*I.n.*), *Bidens pilosa* (*B.p.*), *Commelina benghalensis* (*C.b.*), *Cyperus rotundus (C.r.*), *Amaranthus spinosus* (*A.s.*), *Chenopodium album* (*C.a.*), *Phytolacca Americana* (*P.a.*), *Bidens tripartite* (*B.t.*), *linopodium chinense* (*L.c.*), *Nicandra physaloides* (*N.p.*), *Cassia obtusifolia (C.o.*), *Solanum nigrum* (*S.n.*), and *Vicia gigantean* (*V.g.*) were tested at the concentration of 37.5-150 g ai/ha, using flumioxazin as a control. The inhibition percentages were evaluated at 25 days after treating by compounds, for each treatment, three replications were performed. The herbicidal activity results are shown in Tables 1, 3 and S2.

Crop Selectivity. Six representative crops: wheat, maize, rice, soybean, peanut, and cotton were used in the crop safety experiment.[23, 36] In this test, we evaluated the post-emergence crop safety of all the compounds that showed more than 80% control against at least three of the *E. prostrata*, *A. juncea*, *A. retroflexus*, *S. faberii*, *D. sanguinalis*, and *E. crusgalli* at 37.5 g ai/ha. Flowerpots with 12 cm diameter were filled with mixed soil ($V_{\text{seedling substrate}}$:$V_{\text{vegetable garden soil}}$ = 2:1) to 9 cm depth. Crop seeds were planted and grown at 25 °C (day) and 15 °C (night) in the greenhouse. The application rate for the tested compounds was 150 g ai/ha. The results of crop selectivity (Tables 4 and S3) were evaluated after 25 days of treatment, with three replications per test.

RESULTS AND DISCUSSION

Chemistry. Three similar synthetic routes were designed to synthesize **8**, **9**, **17**, and **19**, which were dependent on the number of n, and the substituents of R^1 and R^2. When n = 1 or 2, R^1 and R^2 are hydrogen atoms, the detailed synthetic routes for **8** and **9** are depicted in Scheme 1; when n = 2, R^1 and R^2 are fluorine atoms, the synthetic routes for **17** are outlined in Scheme 2; when n = 3, R^1 and R^2 are hydrogen atoms, the synthetic routes for **19** are shown in Scheme 3. By using the similar synthetic procedures we have reported, compounds **8** and **9** can be synthesized in 9 to 11 steps.[23] In this work, we found that compounds **8a** and **9a** could be synthesized by a four-step

consecutive reaction. Firstly, **7** reacted with triphosgene in refluxing toluene afforded the corresponding isocyanate, which was directly reacted with ethyl 2-aminocyclopent-1-ene-1-carboxylate or ethyl 2-aminocyclohex-1-ene-1-carboxylate to give the corresponding urea, and got precipitated from the solution upon cooling, without further purification the urea then underwent intramolecular ring closure reactions in CH_3ONa-CH_3OH solution and methylation reaction in DMF with K_2CO_3 as a base to afford **8a** and **9a**. **8b** and **9b** were synthesized by deprotecting the 4-methoxybenzyl groups of **8a** and **9a** in trifluoromethanesulfonic acid and trifluoroacetic acid. **8b** and **9b** reacted with various electrophilic reagents R^3I or R^3Br in DMF with K_2CO_3 as base to give **8c-k** and **9c-l** in yields of 58-88%.

Initial attempts to synthesize **13** by using similar methods as **4** were proved problematic. Ethyl 2,2-difluoro-2-(5-fluoro-2-nitrophenoxy)acetate can be smoothly prepared by reacting of 5-fluoro-2-nitrophenol **1** with ethyl 2-bromo-2,2-difluoroacetate **11** in DMF with K_2CO_3 as a base in 87% yield. We have tried various methods to reduce the nitro group of ethyl 2,2-difluoro-2-(5-fluoro-2- nitrophenoxy)acetate by using H_2/Pd(C), Fe/acetic acid, or Fe/NH_4Cl, and then followed by a ring-closure reaction to obtain **13**. However, the reaction seemed to be unsatisfactory. The reason may be that ethyl 2-(2-amino-5-fluorophenoxy)-2,2-difluoroacetate with two fluorine atoms on α-position of the ether bond significantly reduce the nucleophilic potency of the amino group.

So, another alternative synthetic route shown in Scheme 2 was designed to synthesize **13**. The required intermediate **13** can be synthesized in two steps by reacting of **10** with **11** in tetrahydrofuran with NaH as a base, and then followed by an intramolecular ring closure reaction using Cs_2CO_3 as a base in DMF. Subsequently, **14** was achieved by reacting of **13** with HNO_3 in

concentrated H_2SO_4 in 93% yield. While synthesizing **15** by using a similar method as **6**, the reaction could not proceed due to the weak nucleophilic ability of *NH* group of **14** made it hard to react with 4-methoxybenzyl chloride. 4-methoxybenzyl bromide is more active than 4-methoxybenzyl chloride, therefore, **15** was prepared by reacting 4-methoxybenzyl bromide in DMF with Cs_2CO_3 as a base in a yield of 86%. The fluorine-substituted compounds **17** were obtained in the same fashion as **8** and **9** in yields of 58-86%. Compound **19** was prepared in a yield of 61% with 6-amino-7-fluoro-4-(prop-2-yn-1-yl)-2*H*-benzo[*b*][1,4]oxazin-3(4*H*)-one **18** as the starting material, the synthetic methods were the same as **8a**,**9a**, and **17a**.

PPO Inhibitory Activity and SAR. According to the structural feature of the designed cycloalka[*d*]quinazoline-2,4-dione-benzoxazinones, we intended to optimize it in three ways: one was to explore the size of cycloalkanes ring effect on PPO inhibitory activity; another was to study the substituents change at the 2-positions of benzoxazinone ring (defined as 2-position) effect on activity; the third was to search for the optimum substituents at R^3. Previously, we have reported that for compounds containing of pyrimidine-2,4(1*H*,3*H*)-dione skeleton in their structures, placing a methyl group at the *N*-1-position of pyrimidinedione ring would most favorable to herbicidal activity.[23] Therefore, for the cycloalka[*d*]quinazoline-2,4-dione derivatives, we also kept its *N*-1 position as a methyl group.

Initially, we intended to explore compounds with cyclopropane or cyclobutane ring as the hydrophobic groups that fused to pyrimidine-2,4(1*H*,3*H*)-dione, however, through various synthetic methods were tried, we still could not obtain the needed compounds (data not shown). Compounds containing a cyclopentane ring could be easily synthesized (Scheme 1, compounds **8**). One lead compound, **8a**, was obtained in a yield of 65%, and it showed good PPO inhibition activity with a K_i value of 0.21 μM (Table 1). Inspired by this, we made further optimization of

8a by substituting various groups at the *N*-4-position of benzoxazinone ring (defined as *N*-4-position). It was found that placing a hydrogen atom (**8b**, K_i = 0.34 μM) at this position was detrimental to activity, whereas, placing hydrophobic and medium-chain fatty groups (2-4 carbon atoms) were found favorable to activity. Interesting, compound **8i** with a propargyl group was found to display better PPO inhibition activity comparatively with other substituents at the same position.

Cyclohexane is not only bigger than cyclopentane in size, but also shows more hydrophobicity than cyclopentane. Because introducing the electrostatic positively charged surface at the 6-position of benzoxazinone system is advantageous to activity.[17] Therefore, we envisaged that cyclopentane ring might be a more suitable cycloalkane ring to fuse with pyrimidinedione. The results indicated that in almost all cases, compounds **9** showed higher PPO-inhibiting activity than compounds **8**, which were consistent with our hypothesis. Inspired by this, we decided to change the cyclohexane ring to a seven-membered cycloheptane ring, in order to make further improvement of PPO inhibitory activity. As we have found that the propargyl group was a suitable substituent at R^3 for cyclopentane- and cyclohexane-fused derivatives, **8** and **9**, respectively. Therefore, compound **19** was synthesized. Disappointedly, **19** did not show improved PPO-inhibiting activity than **9i** and **8i** (**9i**, K_i = 0.0067 μM > **8i**, K_i = 0.014 μM > **19**, K_i = 0.072 μM). In addition, it should be noted that efforts to synthesize more membered ring that seven to fuse with pyrimidinedione was proved unsuccessful. Considering the above PPO inhibitory results, we can conclude that the cyclohexane ring was the optimum cycloalkane ring to fuse with pyrimidinedione in the present study.

Having identified the most suitable cycloalkane ring, we then transferred to optimize the substituents at the 2-position. In our previous work, we have demonstrated that introduced methyl

group(s) at this position was detrimental to PPO inhibitory activity, due to the steric clashing between the methyl group(s) with the surrounding residues.[25] These results also suggested that the low substituent tolerance at the 2-position, substituents introduced at this site should be smaller than the methyl group. It is reported that fluorine atom is smaller than methyl group in size, introducing fluorine atom to a compound can increase its hydrophobicity and thermal stability, which in turn can improve its bioactivity.[37-39] Therefore, we introduced two fluorine atoms at the 2-positions. As shown in Table 1, in some cases substituting hydrogen atoms with fluorine atoms were advantageous to the PPO inhibitory activity. For example, the activity of **17h** ($R^1 = R^2 = F$, $K_i = 0.0098$ μM) showed a slightly higher active than its parent compound **9h** ($R^1 = R^2 = H$, $K_i = 0.011$ μM), the propargyl-containing **17i** ($K_i = 0.0067$ μM) was also showed higher PPO-inhibiting activity than **9i** ($K_i = 0.0078$ μM). The promising results demonstrated that introducing the fluorine atoms at 2-positions could improve the binding affinity of inhibitors with PPO.

Though, there was some variation in the SAR of R^3 among compounds **8**, **9** and **17** (Table 1). However, the general trends of substituents changes affected on PPO inhibitory activity still shared some similarity. For examples, substituting the propargyl group (**8i**, **9i**, **17i**) at R^3 was found most favorable to activity; compounds (**8h**, **9h**, **17h**) with allyl groups were also found exhibited very strong PPO-inhibiting activity; placing medium-chain fatty or ester groups at this site was a benefit to activity as well. It should be noted that sometimes even introducing the same group at R^3, the PPO-inhibiting activities of compounds with different motifs still had some variations. In order to understand this molecular basis, we conducted molecular modeling analyses of four representative compounds **8i**, **9i**, **17i**, and **19** with PPO. As shown in Figure 4, there were mainly three similar interactions of **8i**, **9i** and **17i** with surrounding key residues: first,

was the π-π interaction between Phe392 and the pyrimidinedione moieties of the three compounds; second, was the 2.7 Å strong hydrogen bonded interaction between Arg98 and the carbonyl group of benzoxazinone system; and the third, was the sandwich like hydrophobic interactions among benzoxazinone moiety, Leu372, and Leu356. In addition, we found that the binding modes of **8i** and **9i** with NtPPO were almost identical, however, **9i** (K_i = 0.0078 μM) showed higher activity than **8i** (K_i = 0.014 μM). To explain this, we calculated the binding free energies of **8i** and **9i** with NtPPO by using MM-PBSA method. The results showed that the total gas-phase binding energies of **8i** (-76.70 kcal/mol) and **9i** (-76.76 kcal/mol) were almost same (Table S1). However, the higher solvation penalty (**8i** = 39.99 kcal/mol, **9i** = 37.70 kcal/mol) and enthalpy change (**8i** = 9.61 kcal/mol, **9i** = 9.41 kcal/mol) made a lower binding affinity of **8i** (-27.10 kcal/mol) when compared with **9i** (-29.65 kcal/mol), indicating that introduction of cyclohexa[*d*]pyrimidinedione system can reduce the solvation penalty and entropy change and thereby favorable to activity. The fluorine atom of **17i** at 2-position can form a favorable 2.3 Å hydrogen bonding with Gly354 (Figure 4C), indicating that introduced the two fluorine atoms at the 2-position of **9i** could improve its PPO inhibitory activity. Cycloheptane ring is sterically bulky than cyclopentane ring. Hence, as the docking results suggest the binding mode of **19** with PPO was different with that of **8i**, **9i**, and **17i**, due to the steric repulsive effects between the cycloheptane group of **19** and the surrounding residues. Interestingly, though significantly different binding modes were observed in **19**, it still showed acceptable PPO-inhibiting activity (K_i = 0.072 μM). The retained activity of it may attributed to the two hydrogen bonded interaction with Arg98 (3.0 Å) and FAD (2.7 Å).

QSAR Analysis. To elucidate the substitution effect on PPO inhibitory activity of the synthesized compounds, we studied the QSAR of the

cycloalka[*d*]quinazoline-2,4-dione-benzoxazinones, the results of experimental and predicted activity values are listed in Table 2. The conventional coefficient (r^2), cross-validated coefficient (q^2) and noncross-validated coefficient (r^2_{pred}) of the QSAR model are 0.95, 0.66, and 0.83, respectively (Figure 5, Table S4). To better elucidate the QSAR results, compound **17i**, with best PPO-inhibiting activity was selected as a representative and placed in the center of the model (Figure 6). According to the steric contribution contour maps, the green contours mainly located near the *N*-4-position of **17i**, indicating that placing bulky groups at this position was favorable to activity (Figure 6B). For examples, compounds **8c-g**, **9c-g**, and **17c-g** with hydrophobic and medium-chain fatty groups at the *N*-4-position showed higher activity than those with hydrogen atoms substituted compounds **8b**, **9b**, and **17b**, respectively; most of the compounds **9** displayed improved activity than their corresponding compounds **8**. On the contrary, there is almost no yellow polyhedron around **17i**, indicating that placing sterically small groups was not acceptable for activity. For example, substituting a hydrogen atom at R^3 was found detrimental to activity. As shown in Figure 6C, there is almost no red polyhedron around **17i**, indicating that introducing electronegative groups to cycloalka[*d*]quinazolinedione-benzoxazinones have an unfavorable contribution to activity. The blue polyhedrons are situated around the *N*-4-position of **17i** as well, meaning that compounds with electron-positive groups at this position would show high activity. This is consistent with the case of compound **9l** and **17l**, in which, the electronegative nitrogen atom is at the terminal of R^3 showed reduced activity. In contrast, **9i** and **17i** both have electron-positive groups at the terminal of R^3 showed significantly improved activity.

Herbicidal Activity. In the greenhouse tests, we observed that the leaves of sensitive plants became droopy several hours after treating by the tested compounds, followed by bleaching and withering, this process is generally within three days under sunlight. As shown in Table 1, the

herbicidal activities of compounds **8**, **9**, **17**, and **19** correlated well with their PPO-inhibiting activities. In most cases, compounds displayed strong PPO inhibition activity showed higher herbicidal activity as well. Almost all the synthesized compounds displayed nearly 100% inhibition against three broad–leaved weeds (*A. juncea*, *A. retroflexus*, and *E. prostrata*) at the rate of 150 g ai/ha. Nine compounds, **8h**, **8i**, **8k**, **9h**, **9i**, **17h**, **17i**, **17m** and **19**, exhibited at least 4 of the six tested weeds at 150 g ai/ha. It is worth mentioning that, **8i**, **9i**, **17i** and **19** even displayed comparable herbicidal activity to that of flumioxazin and trifludimoxazin against the tested weeds at the 150 g ai/ha.

Due to the excellent herbicidal activity of the synthesized compounds, we performed three rounds of herbicidal evaluation against these compounds. In the first round screening, 37 compounds were tested at the dosage of 150 g ai/ha, a total of 33 compounds (**8b**, **8d-i**, **8k**, **9b-l,** **17** and **19**) showed more than 80% inhibition against at least half of the six tested weeds, most of them exhibited 100% control against the tested broad-leaf weeds (Table 1). Then the 33 compounds were tested at the relative lower concentrations: 75 and 37.5 g ai/ha. The results (Tables 1 and S2) showed that, 29 compounds (**8d-i**, **9b-j**, **9l**, **17b-m** and **19**) exhibited over 80% control against more than three of the six weeds at the concentration of 75 g ai/ha, and 20 compounds (**8d-g**, **8i**, **9c-e**, **9h**, **9i**, and **17b-j**, **17m**) showed more than 80% inhibition against at least three of the tested weeds at 37.5 g ai/ha. Furthermore, 6 compounds **8i**, **9h**, **9i**, **17b** **17h**, and **17i** still exhibited 100% inhibition against three tested broadleaf species at the rate as low as 37.5 g ai/ha. Most promising, **17i** even displayed more than 80% control against the six tested weeds at 37.5 g ai/ha, which were comparable to that of flumioxazin. In most cases, substituting 2 fluorine atoms at the 2-position of compounds can improve their herbicidal activity to some extent. For example, most of compounds **17** showed higher and broader herbicidal actives than

their corresponding mother compounds **9**. We inferred the possible reason is that introducing two fluorine atoms at the 2-positions can increase the lipophilicity of compounds, which will make better absorption of compounds by plant foliage.

Based on the results of the second round screening, three compounds (**8i**, **9i** and **17i**) with excellent and broad-spectrum of weeds control were further evaluated against another 13 kinds of weeds (*I. nil*., *B. pilosa*, *C. benghalensis*, *C. rotundus*, *A. spinosus*, *C. album*, *P. Americana*, *B. tripartite*, *l. chinense*, *N. physaloides*, *C. obtusifolia*, *S. nigrum*, and *V. gigantean*) at the rate of 37.5-150 g ai/ha. A shown in Table 3, all of the three compounds showed more than 80% inhibition against the 13 test weeds at 150 g ai/ha and over 80% control against 12 of 13 test weeds at 75 g ai/ha. At the rate of 37.5 g ai/ha, **8i** showed at least 80% control against 6 kinds of weeds; **9i** displayed more than 80% inhibition against 9 kinds of weeds; **17i** exhibited over 80% inhibition against 12 kinds of weeds, which were comparable to that of flumioxazin, and more potent than that of **9i** and **8i** (**17i** > **9i** > **8i**).

Crop selectivity. 20 compounds (**8d-g**, **8i**, **9c-e**, **9h**, **9i**, and **17b-j**, **17m**) with strong and broad-spectrum of weeds control at 37.5-150 g ai/ha were selected for post-emergent crop safety studies, the results are shown in Tables S3 and 4. Most of the tested compounds displayed no phytotoxicity toward at least one kind of the tested crops at the rate of 150 g ai/ha. For examples, **8d**, **8f**, **9c**, and **9d** exhibited high safety for maize; wheat exhibited relative to high tolerance to **8f**, **8i**, **9d**, **9i**, and **17i**, suggesting the great potential for using these compounds in maize or wheat fields. To our surprise that maize, wheat, and rice showed extremely high tolerance to **17b-h**, **17j**, and **17m**, whereas, flumioxazin and trifludimoxazin were not safe for the six tested crops at the same condition. The promising results indicated that **17b-h**, **17j**, and **17m** had great potential to develop as herbicides application in maize, wheat and rice fields for broad-leaf weeds control.

In summary, we have presented the design, synthesis, herbicidal activity and QSAR studies of cycloalka[*d*]quinazoline-2,4-dione−benzoxazinones as novel PPO inhibitors. The bioassay results indicated that, most of the synthesized compounds exhibited strong PPO inhibition activity; 20 of the 37 synthesized compounds displayed over 80% inhibition against *A. juncea*, *A. retroflexus*, and *E. prostrata* at the rate of 37.5-150 g ai/ha by post-emergence application, most of them exhibited high selectivity toward at least one kind of crop at 150 g ai/ha. Compounds **8i** and **9i** not only exhibited strong and broad-spectrum weeds control comparable to that of flumioxazin at 75-150 g ai/ha, but also showed highly safe to wheat at 150 g ai/ha. Most promisingly, **17i** (K_i = 0.0067 μM) displayed excellent and wide-spectrum herbicidal activity even as low as 37.5 g ai/ha, and relatively safe for wheat at 150 g ai/ha by post-emergent application, indicating the great possibility of **17i** to be a herbicide for weed control in wheat fields. Furthermore, a highly predictive QSAR model was built to understand the activity of the newly synthesized compounds. The results showed that the highest activity is obtained for inhibitors with cyclohexa[*d*]pyrimidine-2,4-dione moiety at the 6-position of benzoxazinone ring, hydrophobic and medium-sized groups at the *N*-4-position. The molecular docking analyses revealed that placing fluorine atoms at the 2-position was advantageous to activity by forming the fluorine atom mediated hydrogen binding with the surrounding residues. Our present study not only provides a series of potential candidates for herbicide discovery but also be useful for the design and development of novel benzoxazinone-containing compounds.

Supporting Information

The detailed synthetic routes, ^{1}H and ^{13}C NMR and HRMS spectra of compounds **8**, **9**, **17** and **19**; calculated binding free energies of **8i** and **9i** with NtPPO (Table S1), post-emergence herbicidal

activity of compounds **8b**, **8d-g**, **9b-g**, **9j-l**, **17a-g** and **17j-l** at 37.5-75 g ai/ha (Table S2); post-emergence crop selectivity of compounds **8d-g**, **9c-e**, **9h**, **17b-h**, **17j**, and **17m** at 150 g ai/ha (Table S3); and statistical data of 3D-QSAR model (Table S4) are shown in the Supporting Information.

Acknowledgment

This research was funded in part by the National Key Research and Development Program of China (No. 2017YFD0200501), the National Natural Science Foundation of China (No. 21702111, 21672118, 21332004), the Tianjin Natural Science Foundation (No. 16JCYBJC20200), and the China Postdoctoral Science Foundation Funded Project (No. 2016M591384).

Notes

The authors declare no competing financial interest.

REFERENCES

(1) Zhang, F.; Tang, W.; Hedtke, B.; Zhong, L.; Liu, L.; Peng, L.; Lu, C.; Grimm, B.; Lin, R., Tetrapyrrole biosynthetic enzyme protoporphyrinogen IX oxidase 1 is required for plastid RNA editing. *Proc. Natl. Acad. Sci. U. S. A.* **2014**, *111*, 2023-2028.

(2) Patzoldt, W. L.; Hager, A. G.; McCormick, J. S.; Tranel, P. J., A codon deletion confers resistance to herbicides inhibiting protoporphyrinogen oxidase. *Proc. Natl. Acad. Sci. USA* **2006**, *103*, 12329-12334.

(3) Hao, G. F.; Tan, Y.; Xu, W. F.; Cao, R. J.; Xi, Z.; Yang, G. F., Understanding resistance

mechanism of protoporphyrinogen oxidase-inhibiting herbicides: insights from computational mutation scanning and site-directed mutagenesis. *J. Agric. Food Chem.* **2014**, *62*, 7209-7215.

(4) Powles, S. B.; Yu, Q., Evolution in action: plants resistant to herbicides. *Annu. Rev. Plant Biol.* **2010**, *61*, 317-347.

(5) Tan, Y.; Sun, L.; Xi, Z.; Yang, G. F.; Jiang, D. Q.; Yan, X. P.; Yang, X.; Li, H. Y., A capillary electrophoresis assay for recombinant *Bacillus subtilis* protoporphyrinogen oxidase. *Anal. Biochem.* **2008**, *383*, 200-204.

(6) Qin, X. H.; Sun, L.; Wen, X.; Yang, X.; Tan, Y.; Jin, H.; Cao, Q. Y.; Zhou, W. H.; Xi, Z.; Shen, Y. Q., Structural insight into unique properties of protoporphyrinogen oxidase from *Bacillus subtilis*. *J. Struct. Biol.* **2010**, *170*, 76-82.

(7) Wang, B. F.; Wen, X.; Qin, X. H.; Wang, Z. F.; Tan, Y.; Shen, Y. Q.; Xi, Z., Quantitative structural insight into human variegate porphyria disease. *J. Biol. Chem.* **2013**, *288*, 11731-11740.

(8) Green, J. M.; Owen, M. D., Herbicide-resistant crops: utilities and limitations for herbicide-resistant weed management. *J. Agric. Food Chem.* **2011**, *59*, 5819-5829.

(9) Selby, T. P.; Ruggiero, M.; Hong, W.; Travis, D. A.; Satterfield, A. D.; Ding, A. X., Broad-spectrum PPO-inhibiting *N*-phenoxyphenyluracil acetal ester herbicides. *ACS Symp. Ser.* **2015**, *1204*, 277-289.

(10) Jeanmart, S.; Edmunds, A. J.; Lamberth, C.; Pouliot, M., Synthetic approaches to the 2010-2014 new agrochemicals. *Bioorg. Med. Chem.* **2016**, *24*, 317-341.

(11) Park, J.; Ahn, Y. O.; Nam, J. W.; Hong, M. K.; Song, N.; Kim, T.; Yu, G. H.; Sung, S. K., Biochemical and physiological mode of action of tiafenacil, a new protoporphyrinogen IX oxidase-inhibiting herbicide. *Pestic. Biochem. Physiol.* **2018**, *152,* 38-44.

(12) Hao, G. F.; Zuo, Y.; Yang, S. G.; Yang, G. F., Protoporphyrinogen oxidase inhibitor: an ideal target for herbicide discovery. *Chimia* **2011**, *65*, 961-969.

(13) Grossmann, K.; Hutzler, J.; Caspar, G.; Kwiatkowski, J.; Brommer, C. L., Saflufenacil (Kixor™): biokinetic properties and mechanism of selectivity of a new protoporphyrinogen IX oxidase inhibiting herbicide. *Weed Sci.* **2011**, *59*, 290-298.

(14) Leet, J. K.; Hipszer, R. A.; Volz, D. C., Butafenacil: A positive control for identifying anemia- and variegate porphyria-inducing chemicals. *Toxicol. Rep.* **2015**, *2*, 976-983.

(15) Beam, S. C.; Chaudhari, S.; Jennings, K. M.; Monks, D. W.; Meyers, S. L.; Schultheis, J. R.; Waldschmidt, M.; Main, J. L., Response of palmer amaranth and sweetpotato to flumioxazin/pyroxasulfone. *Weed Technol.* **2018**, *33*, 128-134.

(16) Macias, F. A.; Marin, D.; Oliveros-Bastidas, A.; Molinillo, J. M. G., Optimization of benzoxazinones as natural herbicide models by lipophilicity enhancement. *J. Agric. Food Chem.* **2006**, *54*, 9357-9365.

(17) Roy, K.; Paul, S., Docking and 3D QSAR studies of protoporphyrinogen oxidase inhibitor 3*H*-pyrazolo[3,4-*d*][1,2,3]triazin-4-one derivatives. *J Mol Model* **2010**, *16*, 137-153.

(18) Huang, M. Z.; Luo, F. X.; Mo, H. B.; Ren, Y. G.; Wang, X. G.; Ou, X. M.; Lei, M. X.; Liu, A. P.; Huang, L.; Xu, M. C., Synthesis and herbicidal activity of isoindoline-1,3-dione substituted benzoxazinone derivatives containing a carboxylic ester group. *J. Agric. Food Chem.* **2009**, *57*, 9585-9892.

(19) Wang, B. F.; Wen, X.; Xi, Z., Molecular simulations bring new insights into protoporphyrinogen IX oxidase/protoporphyrinogen IX interaction modes. *Mol Inform* **2016**, *35*, 476-482.

(20) Fan, Y. Y.; Gao, X. H.; Yue, J. M., Attractive natural products with strained cyclopropane and/or cyclobutane ring systems. *Sci. China Chem.* **2016**, *59*, 1126-1141.

(21) Song, L.; Merceron, R.; Gracia, B.; Quintana, A. L.; Risseeuw, M. D. P.; Hulpia, F.; Cos, P.; Ainsa, J. A.; Munier-Lehmann, H.; Savvides, S. N.; Van Calenbergh, S., Structure guided lead generation toward nonchiral *M. tuberculosis* thymidylate kinase inhibitors. *J. Med. Chem.* **2018**, *61*, 2753-2775.

(22) Wiesenfeldt, M. P.; Nairoukh, Z.; Li, W.; Glorius, F., Hydrogenation of fluoroarenes: Direct access to all-*cis*-(multi)fluorinated cycloalkanes. *Science* **2017**, *357*, 908-912.

(23) Wang, D. W.; Li, Q.; Wen, K.; Ismail, I.; Liu, D. D.; Niu, C. W.; Wen, X.; Yang, G. F.; Xi, Z., Synthesis and herbicidal activity of pyrido[2,3-*d*]pyrimidine-2,4-dione-benzoxazinone hybrids as protoporphyrinogen oxidase inhibitors. *J. Agric. Food Chem.* **2017**, *65*, 5278-5286.

(24) Zuo, Y.; Wu, Q.; Su, S. W.; Niu, C. W.; Xi, Z.; Yang, G. F., Synthesis, herbicidal activity, and QSAR of novel *N*-benzothiazolyl-pyrimidine-2,4-diones as protoporphyrinogen oxidase inhibitors. *J. Agric. Food Chem.* **2016**, *64*, 552-562.

(25) Hao, G. F.; Zuo, Y.; Yang, S. G.; Chen, Q.; Zhang, Y.; Yin, C. Y.; Niu, C. W.; Xi, Z.; Yang, G. F., Computational discovery of potent and bioselective protoporphyrinogen IX oxidase inhibitor via fragment deconstruction analysis. *J. Agric. Food Chem.* **2017**, *65*, 5581-5588.

(26) Morris, G. M.; Huey, R.; Lindstrom, W.; Sanner, M. F.; Belew, R. K.; Goodsell, D. S.; Olson, A. J., AutoDock4 and AutoDockTools4: Automated docking with selective receptor flexibility. *J. Comput. Chem.* **2009**, *30*, 2785-2791.

(27) Koch, M.; Breithaupt, C.; Kiefersauer, R.; Freigang, J.; Huber, R.; Messerschmidt, A., Crystal structure of protoporphyrinogen IX oxidase: a key enzyme in haem and chlorophyll biosynthesis. *EMBO J.* **2004**, *23*, 1720-1728.

(28) Tosco, P.; Balle, T.; Shiri, F. Open3DALIGN: an opensource software aimed at

471 unsupervised ligand alignment, *J Comput Aid Mol Des.* **2011**, *25*,777-783.

472 (29) Tosco, P.; Balle, T., Open3DQSAR: a new open-source software aimed at high-throughput
473 chemometric analysis of molecular interaction fields. *J Mol Model* **2011**, *17*, 201-208.

474 (30) Jiang, L. L.; Ying, T.; Zhu, X. L.; Wang, Z. F.; Yang, Z.; Qiong, C.; Zhen, X.; Yang, G. F.,
475 Design, synthesis, and 3D-QSAR analysis of novel 1,3,4-oxadiazol-2(3*H*)-ones as
476 protoporphyrinogen oxidase inhibitors. *J. Agric. Food Chem.* **2010**, *58*, 2643-2651.

477 (31) Wang, D. W.; Lin, H. Y.; Cao, R. J.; Yang, S. G.; Chen, T.; He, B.; Chen, Q.; Yang, W. C.;
478 Yang, G. F., Synthesis and bioactivity studies of triketone-containing quinazoline-2,4-dione
479 derivatives. *Huaxue Xuebao.* **2015**, *73*, 29-35.

480 (32) Wang, D. W.; Lin, H. Y.; Cao, R. J.; Chen, T.; Wu, F. X.; Hao, G. F.; Chen, Q.; Yang, W.
481 C.; Yang, G. F., Synthesis and herbicidal activity of triketone-quinoline hybrids as novel
482 4-hydroxyphenylpyruvate dioxygenase inhibitors. *J. Agric. Food Chem.* **2015**, *63*,
483 5587-5596.

484 (33) Wang, D. W.; Lin, H. Y.; Cao, R. J.; Yang, S. G.; Chen, Q.; Hao, G. F.; Yang, W. C.;
485 Yang, G. F., Synthesis and herbicidal evaluation of triketone-containing
486 quinazoline-2,4-diones. *J. Agric. Food Chem.* **2014**, *62*, 11786-11796.

487 (34) Wang, D. W.; Lin, H. Y.; He, B.; Wu, F. X.; Chen, T.; Chen, Q.; Yang, W. C.; Yang, G. F.,
488 An efficient one-pot synthesis of 2-(aryloxyacetyl)cyclohexane-1,3-diones as herbicidal
489 4-hydroxyphenylpyruvate dioxygenase inhibitors. *J. Agric. Food Chem.* **2016**, *64*,
490 8986-8993.

491 (35) Wang, D. W.; Lin, H. Y.; Cao, R. J.; Ming, Z. Z.; Chen, T.; Hao, G. F.; Yang, W. C.; Yang,
492 G. F., Design, synthesis and herbicidal activity of novel quinazoline-2,4-diones as
493 4-hydroxyphenylpyruvate dioxygenase inhibitors. *Pest Manag. Sci.* **2015**, *71*, 1122-1132.

494 (36) Jiang, L. L.; Zuo, Y.; Wang, Z. F.; Tan, Y.; Wu, Q. Y.; Xi, Z.; Yang, G. F., Design and

syntheses of novel *N*-(benzothiazol-5-yl)-4,5,6,7-tetrahydro-1*H*-isoindole-1,3(2*H*)-dione and *N*-(benzothiazol-5-yl)isoindoline-1,3-dione as potent protoporphyrinogen oxidase inhibitors. *J. Agric. Food Chem.* **2011**, *59*, 6172-6179.

(37) Smart, B. E., Fluorine substituent effects (on bioactivity). *J. Fluorine Chem.* **2001**, *109*, 3-11.

(38) Liang, Z.; Li, Q. X., π-cation interactions in molecular recognition: perspectives on pharmaceuticals and pesticides. *J. Agric. Food Chem.* **2018**, *66*, 3315-3323.

(39) Jeffries, B.; Wang, Z.; Graton, J.; Holland, S. D.; Brind, T.; Greenwood, R. D. R.; Le Questel, J. Y.; Scott, J. S.; Chiarparin, E.; Linclau, B., Reducing the lipophilicity of perfluoroalkyl groups by CF_2-F/CF_2-Me or CF_3/CH_3 exchange. *J. Med. Chem.* **2018**, *61*, 10602-10618.

Figure and Scheme Captions:

Figure 1. Chemical structures of some commercial PPO herbicides and the synthesized compounds **8**, **9**, **17**, and **19**.

Figure 2. Design protocol of novel cycloalka[*d*]quinazolinedione-benzoxazinones.

Figure 3. Crystal structure of compound **17a**.

Figure 4. Simulated binding modes of **8i**, **9i**, **17i**, and **19** with NtPPO. The key residues around the active site are shown in blue sticks, (A) Binding mode of **8i** with NtPPO; (B) Binding mode of **9i** with NtPPO; (C) Binding mode of **17i** with NtPPO; (D) Binding mode of **19** with NtPPO.

Figure 5. Correlation of experimental and predicted pK_i values.

Figure 6. (**A**) Alignment of 28 training set compounds. (B) Contour maps of steric contribution, compound **17i** is located in the center of the filed. (C) Contour maps of electrostatic contribution, compound **17i** is located in the center of the filed.

Scheme 1. Synthesis of compounds **8** and **9**. Reagents and conditions: (a) K_2CO_3, DMF, r.t.; (b) Fe, acetic acid, reflux; (c) HNO_3, H_2SO_4, 0 °C-r.t.; (d) 4-methoxybenzyl chloride (PMBCl), K_2CO_3, DMF, r.t.; (e) Fe, NH_4Cl, C_2H_5OH (90%), reflux; (f) $CO(OCCl_3)_2$, Et_3N, toluene, 0 °C to reflux; (g) ethyl 2-aminocyclopent-1-ene-1-carboxylate or ethyl 2-aminocyclohex-1-ene-1-carboxylate, toluene, reflux; (h) $NaOCH_3$, CH_3OH, r.t.; (i) CH_3I, K_2CO_3, DMF, r.t.; (j) CF_3SO_3H, CF_3CO_2H, CH_2Cl_2, r.t.; (k) R^3Br or R^3I, K_2CO_3, DMF, r.t..

Scheme 2. Synthesis of compounds **17**. Reagents and conditions: (a) NaH, THF, -15 °C - r.t.; (b) Cs_2CO_3, DMF, 75 °C; (c) HNO_3, H_2SO_4, -10 °C-r.t.; (d) 4-methoxybenzyl bromide (PMBBr), Cs_2CO_3, DMF, r.t.; (e) Fe, NH_4Cl, C_2H_5OH (90%), reflux; (f) $CO(OCCl_3)_2$, Et_3N, toluene, 0 °C to reflux; (g) ethyl 2-aminocyclohex-1-ene-1-carboxylate, toluene, reflux; (h) $NaOCH_3$, CH_3OH, r.t.; (i) CH_3I, K_2CO_3, DMF, r.t.; (j) CF_3SO_3H, CF_3CO_2H, CH_2Cl_2, r.t.; (k) R^3Br or R^3I, K_2CO_3, DMF, r.t..

Scheme 3. Synthesis of compound **19**. Reagents and conditions: (a) $CO(OCCl_3)_2$, Et_3N, toluene, 0 °C to r.t.; (b) toluene, reflux; (c) $NaOCH_3$, CH_3OH, r.t.; (d) CH_3I, K_2CO_3, DMF, r.t..

Tables:

Table 1. Post-emergence herbicidal activity and NtPPO inhibitory activity of compounds **8**, **9**, **17**, and **19.**

compds	n	R^1	R^2	R^3	dosage g ai/ha	% inhibition						$K_i/\mu M^b$
						A.j.[a]	*A.r.*	*E.p.*	*D.s.*	E.c.	*S.f.*	
8a	1	H	H	$CH_2C_6H_4(4\text{-}OCH_3)$	150	30	80	30	0	0	0	0.21
8b	1	H	H	H	150	100	80	80	0	0	0	0.34
8c	1	H	H	CH_3	150	100	50	80	0	0	0	0.27
8d	1	H	H	CH_2CH_3	150	100	100	100	0	0	0	0.098
8e	1	H	H	$CH_2CH_2CH_3$	150	100	100	100	0	0	0	0.069
8f	1	H	H	$CH_2CH_2CH_2CH_3$	150	100	100	90	0	0	0	0.12
8g	1	H	H	$CH_2CH(CH_3)_2$	150	100	100	100	0	0	0	0.17
8h	1	H	H	$CH_2CH{=}CH_2$	150	100	100	100	80	0	80	0.020
					75	100	80	100	30	30	30	
					37.5	100	40	80	0	0	0	
8i	1	H	H	$CH_2C{\equiv}CH$	150	100	100	100	90	100	100	0.014
					75	100	100	100	50	85	70	
					37.5	100	100	100	30	80	30	
8j	1	H	H	$CH_2C{\equiv}CSi(CH_3)_3$	150	100	100	70	0	0	0	2.50
8k	1	H	H	$CH_2CO_2CH_2CH_3$	150	80	80	80	0	0	80	0.048
					75	60	50	80	0	30	60	
					37.5	50	30	70	0	0	0	
9a	2	H	H	$CH_2C_6H_4(4\text{-}OCH_3)$	150	70	70	70	0	0	0	0.20
9b	2	H	H	H	150	100	100	100	0	0	0	0.21
9c	2	H	H	CH_3	150	100	100	100	45	50	45	0.16
9d	2	H	H	CH_2CH_3	150	100	100	100	0	0	0	0.098
9e	2	H	H	$CH_2CH_2CH_3$	150	100	100	100	50	50	50	0.044
9f	2	H	H	$CH_2CH_2CH_2CH_3$	150	100	100	100	0	0	0	0.046
9g	2	H	H	$CH_2CH(CH_3)_2$	150	100	100	100	0	0	0	0.10
9h	2	H	H	$CH_2CH{=}CH_2$	150	100	100	100	80	80	80	0.011
					75	100	100	100	30	30	30	
					37.5	100	100	100	0	0	0	
9i	2	H	H	$CH_2C{\equiv}CH$	150	100	100	100	100	100	100	0.0078
					75	100	100	100	80	90	80	
					37.5	100	100	100	60	70	60	
9j	2	H	H	$CH_2C{\equiv}CSi(CH_3)_3$	150	100	100	90	0	0	0	0.26
9k	2	H	H	$CH_2CO_2CH_2CH_3$	150	100	100	100	0	0	0	0.037
9l	2	H	H	CH_2CN	150	100	100	100	0	0	0	0.11
17a	2	F	F	$CH_2C_6H_4(4\text{-}OCH_3)$	150	100	100	80	0	0	0	0.20
17b	2	F	F	H	150	100	100	100	50	50	50	0.48
17c	2	F	F	CH_3	150	100	100	100	30	30	30	0.14
17d	2	F	F	CH_2CH_3	150	100	100	100	0	0	0	0.11
17e	2	F	F	$CH_2CH_2CH_3$	150	100	100	100	60	60	60	0.058
17f	2	F	F	$CH_2CH_2CH_2CH_3$	150	100	100	100	60	60	60	0.021

17g	2	F	F	$CH_2CH(CH_3)_2$	150	100	100	90	0	0	0	0.084
17h	2	F	F	$CH_2CH=CH_2$	150	100	100	100	50	80	70	0.0098
					75	100	100	100	40	70	60	
					37.5	100	100	100	30	30	30	
17i	2	F	F	$CH_2C\equiv CH$	150	100	100	100	100	90	100	0.0067
					75	100	100	100	90	85	90	
					37.5	100	100	100	80	80	80	
17j	2	F	F	$CH_2C\equiv CSi(CH_3)_3$	150	100	100	90	0	0	0	0.17
17k	2	F	F	CH_2CO_2Et	150	100	100	85	0	0	0	0.014
17l	2	F	F	CH_2CN	150	100	100	100	0	0	0	0.20
17m	2	F	F	$CH_2CH_2OCH_3$	150	100	100	100	80	80	80	0.12
					75	100	100	85	50	50	50	
					37.5	100	100	80	30	30	30	
19	3	F	F	$CH_2C\equiv CH$	150	100	100	100	100	100	100	0.072
					75	100	90	80	50	50	50	
					37.5	100	40	50	0	0	0	
flumioxazin					150	100	100	100	100	100	95	0.046
					75	100	100	100	95	95	80	
					37.5	100	100	100	90	80	70	
trifludimoxazin					150	100	100	100	100	100	100	0.031
					75	100	100	100	100	100	100	
					37.5	100	100	100	95	100	100	

[a]Abbreviations: *A.j.*, *Abutilon juncea*; *A.r.*, *Amaranthus retroflexus*; *E.P.*, *Eclipta prostrata*; *D.s.*, *Digitaria sanguinalis*; *E.C.*, *Echinochloa crusgalli*; *S.f.*, *Setaria faberii*.

539 Table 2. Experimental and Calculated pK_i Values of Compounds **8**, **9**, **17**, and **19.**

compds	pK_i[a]		compds	pK_i[a]	
	exptl	calcd		exptl	calcd
8a	6.68	6.61	**9i**	8.11	8.27
8b[b]	6.77	6.54	**9j**	6.77	6.91
8c	6.57	6.57	**9k**	7.43	7.37
8d[b]	7.01	6.80	**9l**	7.43	7.23
8e	7.16	7.11	**17a**	6.68	6.67
8f	6.92	6.95	**17b**	6.32	6.35
8g	6.77	6.82	**17c**[b]	6.86	6.54
8h[b]	7.70	7.45	**17d**	6.96	6.84
8i	7.85	7.94	**17e**	7.24	7.18
8k	7.32	7.15	**17f**[b]	6.70	6.89
9a	6.70	6.75	**17g**	7.08	7.18
9b[b]	7.00	6.90	**17h**	8.01	7.83
9c[b]	6.80	6.91	**17i**	8.17	7.98
9d	7.01	7.16	**17j**	6.82	6.73
9e	7.36	7.43	**17k**	7.85	7.99
9f	7.34	7.25	**17l**	6.70	6.92
9g	7.00	7.00	**17m**	6.92	7.01
9h	7.96	7.93	**19**[b]	8.17	8.13

540 [a]p$K_i = -\log K_i$, [b]test set compunds.

541

542 Table 3. Herbicidal spectrum of compounds **8i**, **9i, and 17i** (post-emergence)**.**

compds	dosage	% inhibition												
	g ai/ha	*I.n.*[a]	*B.p.*	*C.b.*	*C.r.*	*A.s.*	*C.a.*	*P.a.*	*B.t.*	*L.c.*	*N.p.*	*C.o.*	*S.n.*	*V.g.*
8i	150	95	100	100	95	85	100	95	95	100	100	95	100	100
	75	90	100	100	90	80	100	75	90	95	100	90	100	80
	37.5	75	100	70	70	75	100	70	90	60	100	80	100	50
9i	150	100	100	100	90	90	100	95	95	100	100	100	100	100
	75	95	100	100	80	70	100	85	90	100	100	95	100	100
	37.5	85	100	95	60	50	60	80	80	90	100	80	100	70
17i	150	100	100	100	80	100	100	100	100	100	100	100	100	100
	75	95	100	100	75	90	100	95	90	100	100	95	100	90
	37.5	90	100	95	70	80	100	80	90	90	100	80	100	85
flumioxazin	150	100	100	100	90	100	100	100	100	100	100	100	100	100
	75	100	100	100	85	100	100	100	100	100	100	100	100	100
	37.5	100	100	100	80	100	100	100	80	100	100	100	100	100

543 [a]Abbreviations: *I.n.*, *Ipomoea nil*; *B.p.*, *Bidens pilosa*; *C.b.*, *Commelina benghalensis*; *C.r.*,
544 *Cyperus rotundus*; *A.s.*, *Amaranthus spinosus*; *C.a.*, *Chenopodium album*; *P.a.*; *Phytolacca*
545 *Americana*; *B.t.*, *Bidens tripartite*; *L.c.*, *linopodium chinense*; *N.p.*, *Nicandra physaloides*; *C.o.*,
546 *Cassia obtusifolia*; *S.n.*, *Solanum nigrum*; *V.g.*, *Vicia gigantean.*
547

548 Table 4. Crop Selectivity of compounds **8i**, **9i**, and **17i** (post-emergence, 150 g ai/ha).

compds	% injury					
	wheat	maize	rice	peanut	cotton	soybean
8i	10	15	40	40	70	80
9i	10	15	50	50	70	80
17i	20	30	50	50	70	80
flumioxazin	70	60	80	80	80	80
trifludimoxazin	100	80	90	100	100	100

549

550

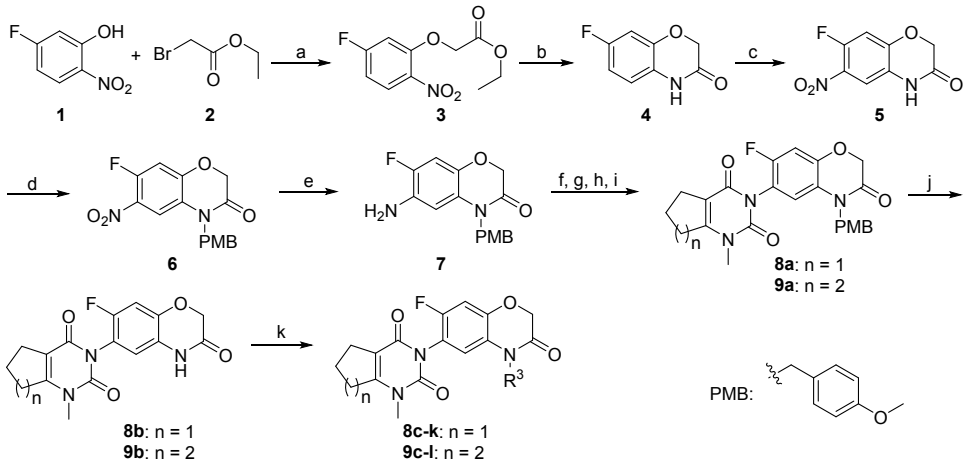

551

552 **Scheme 1**.

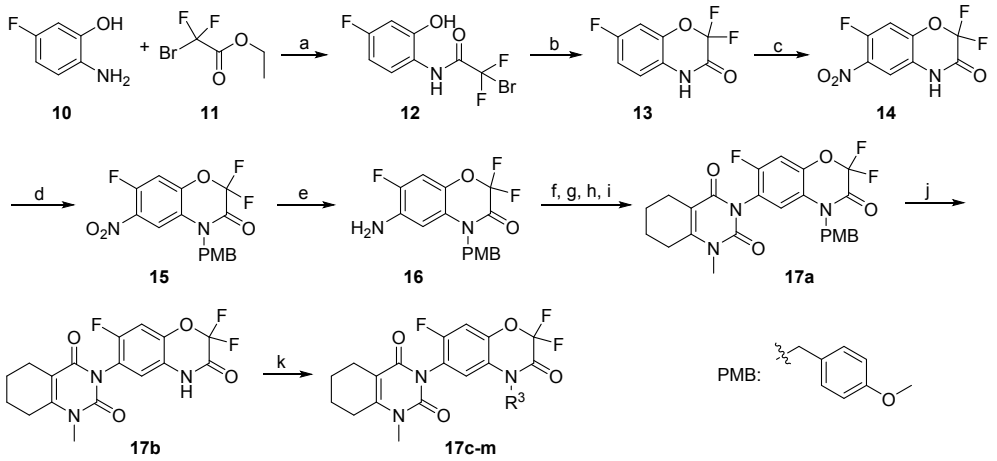

Scheme 2.

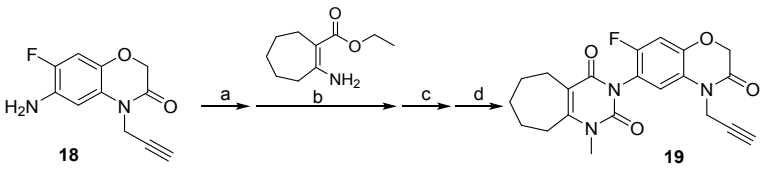

Scheme 3.

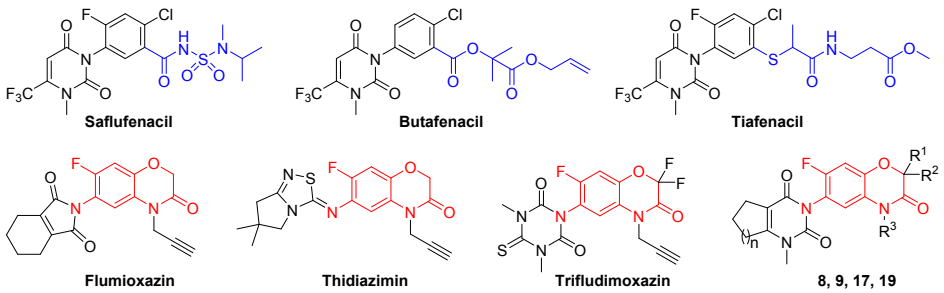

562

563 **Figure 1**

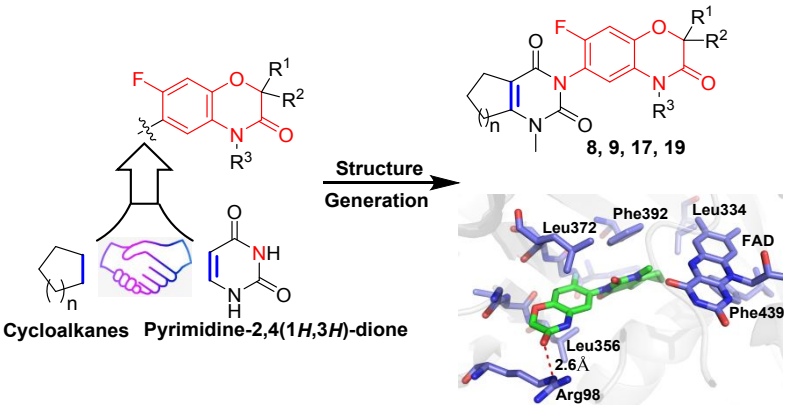

564

565 **Figure 2.**

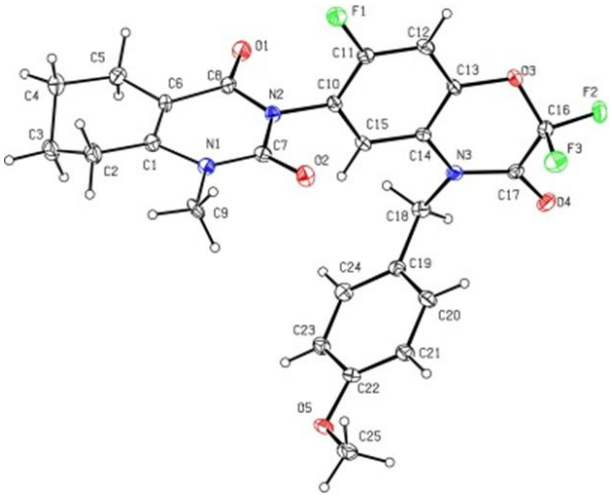

566

567 **Figure 3.**

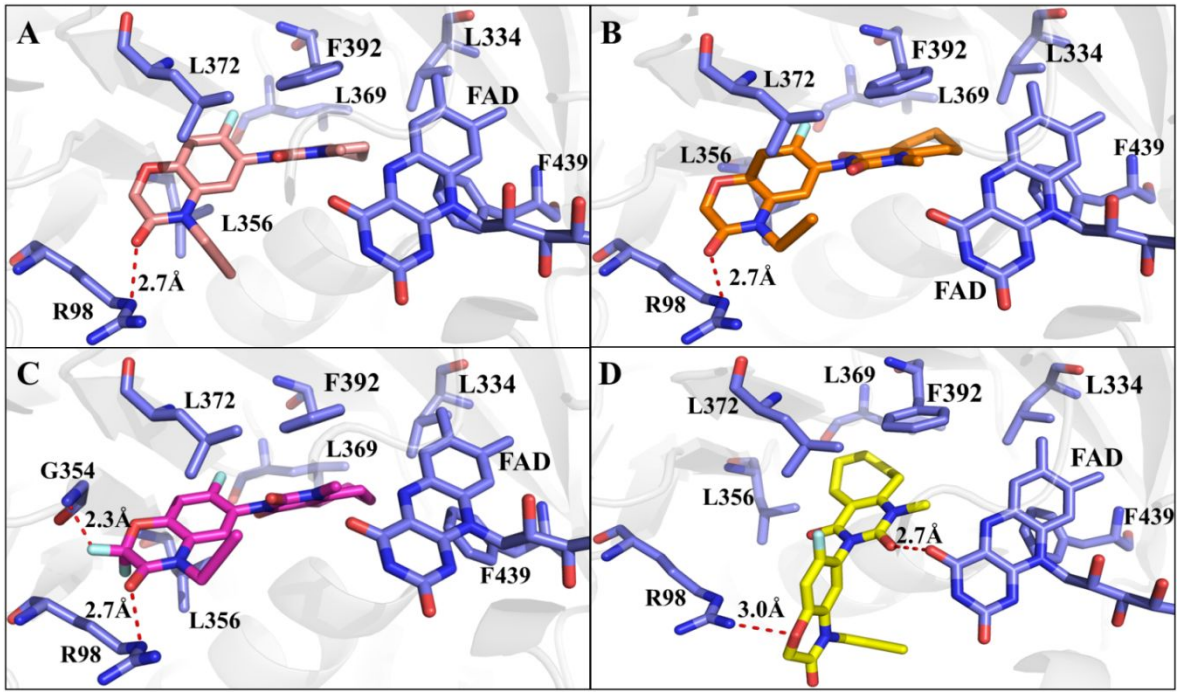

568

569 **Figure 4.**

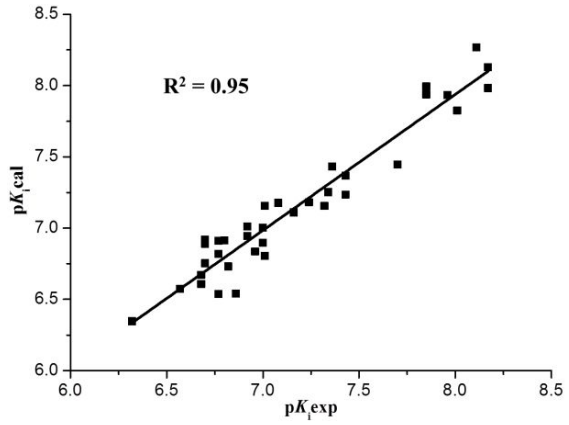

570

571 **Figure 5.**

572

573

574

575

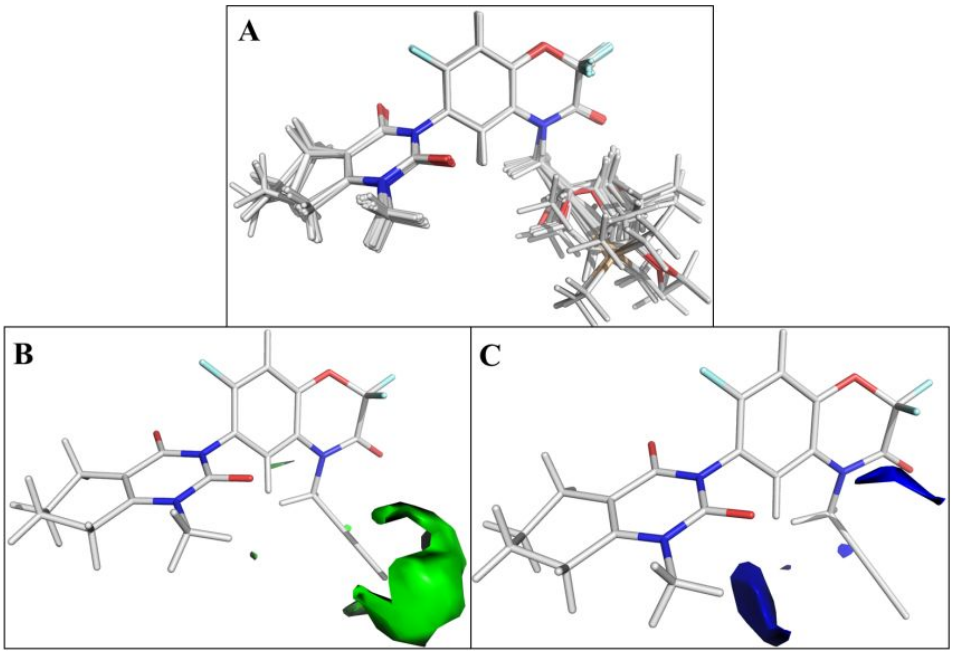

576

577 **Figure 6.**

578 **Table of Contents Graphic**

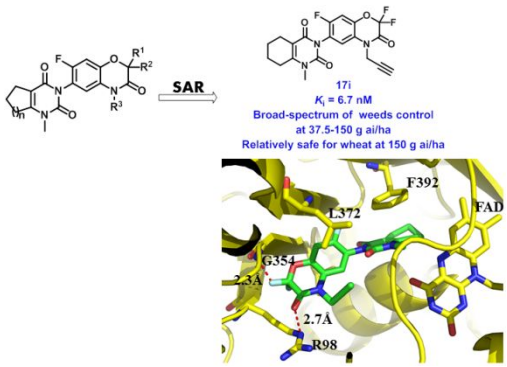

579